Experimental investigation on the monotonic and cyclic behaviour of a structured clay at high confinement

Experimental investigation on the monotonic and cyclic behaviour of a structured clay at high confinement

by

Andrea Ciancimino[1*], Renato Maria Cosentini[2], Sebastiano Foti[3], Giorgio Volonté[4], Guido Musso[5]

[1*]Corresponding author, Politecnico di Torino, Turin, Italy; andrea.ciancimino@polito.it; 0000-0001-8955-4605
[2]Politecnico di Torino, Turin, Italy; renato.cosentini@polito.it; 0000-0002-7080-2186
[3]Politecnico di Torino, Turin, Italy; sebastiano.foti@polito.it; 0000-0003-4505-5091
[4]Eni SpA, Milan, Italy; giorgio.volonte@eni.com; 0000-0002-6942-7198
[5]Politecnico di Torino, Turin, Italy; guido.musso@polito.it; 0000-0003-3151-4058

Abstract

In this paper, the monotonic and cyclic behaviour of a structured clay is experimentally evaluated by means of anisotropically consolidated undrained triaxial tests. The material behaviour under high confinement pressure is analysed with a view to underground gas storage applications by imposing one-way fatigue loads characterized by large periods. The experimental results highlight the role of the material structure and the consequences of its progressive degradation, which implies a fragile stress-strain response. The results also show the relevance of time-dependent effects. Under monotonic strain-controlled conditions, such effects induce a strong strain rate dependence of the peak strength. Under cyclic stress-controlled loading, the fatigue life is shown to be influenced by the loading period and the characteristics of the sinusoidal history. Longer loading periods result in a lower number of cycles to failure. Similarly, larger maximum imposed deviatoric stresses also result in a reduction in fatigue life. Conversely, a somewhat counter-intuitive response is observed in tests carried out with the same maximum imposed deviatoric stress, since an increase in loading amplitude implies an increase in the number of cycles to failure. The reasons for the observed results are discussed in detail in the light of the peculiarities of the material response.

Keywords

fabric/structure of soils; cyclic loading; time dependence; fatigue; laboratory tests

1 Introduction

Experimental evidence has shown that the mechanical response of natural clays is governed by their microstructural features, which confer to the material a lower compressibility before yielding and a larger shear strength than those observed in the corresponding reconstituted soil (e.g., Burland, 1990; Leroueil & Vaughan, 1990; Cotecchia & Chandler, 1997). These differences are attributed to the 'structure' of the material in its undisturbed state, resulting from a combination of 'fabric' (i.e. the arrangement of soil particles, e.g., Ladd, 1965; Parry & Nadarajah, 1974) and interparticle 'bonding' (e.g. Gens, 2013). The structure is therefore the result of both sedimentation and post-sedimentation processes (Cotecchia & Chandler, 2000).

The role of structure has been widely reported in the past, both in terms of volumetric and deviatoric responses. Under oedometric compression, this role can be exploited by using the 'intrinsic' compression line as a reference, i.e. the line associated with the admissible states for a normally-consolidated, reconstituted clay in the void ratio – effective vertical stress $e - \log\sigma'_v$ plane (after Burland, 1990). The state of a natural, normally-consolidated clay not affected by post-sedimentation effects typically lies above the intrinsic compression line, on the so-called 'sedimentation' compression line (Terzaghi, 1941; Skempton, 1969). Consequently, the admissible state space for natural clay is extended compared to that for reconstituted clay due to its natural fabric (Leroueil & Vaughan, 1990). After deposition, cementation and lithification processes can occur, leading to the development of interparticle bonding (e.g. Cotecchia & Chandler, 1997). The degree of bonding can impart a substantial structure to natural clays, so they can be considered as transitional materials between rocks and soils in terms of strength, porosity and compressibility (Clayton & Serratrice, 1993). Upon reloading, bonded geomaterials are expected to exhibit a consolidation curve that crosses the sedimentation line before yield stress is reached (Burland et al., 1996). After yielding, progressive destructuration typically occurs. This is manifested, for example, by an increase in the slope of the swelling line, as has been shown for several structured clays (e.g., Banks et al., 1975; Gasparre et al., 2007; Mohajerani et al., 2011). The structure degradation implies a reduction in the yield stress with a consolidation path tending towards the intrinsic compression line. However, the response of natural clays does not always converge to the reconstituted one (e.g. Amorosi & Rampello, 2007). This can be explained by referring to the distinction proposed by Baudet and Stallebrass (2004) between 'stable' and 'metastable' structures. A stable structure is mainly associated with the natural fabric, which evolves after yielding, but does not necessarily tend towards the intrinsic one. Instead, metastability is more likely to result from interparticle debonding, an irreversible process that occurs when the interparticle contact forces approach the bond strength. This type of degradation is controlled by inelastic strain

accumulation and often results in a fragile mechanical response, tending towards a fully debonded state (e.g., Smith et al., 1992).

Under monotonic shear, structured clays are characterised by a stiff response up to the peak strength, followed by a pronounced softening and then a gradual reduction in strength. Experimentally, this behaviour has been observed in direct shear tests (e.g., Bardanis, 2024) and in triaxial tests (e.g., Leroueil & Vaughan, 1990; Burland et al., 1996). The initial steep decrease to the so-called post-rupture strength is mainly associated with interparticle debonding, whereas the second stage can be considered as an effect of the fabric evolution (Burland, 1990). Brittle failure is typically associated with the progressive development of a sharp shear band within the specimen. A more ductile response can be observed for the same materials when consolidated up to large confinements (i.e., larger than in situ), although brittle failure is most likely to develop in conventional geotechnical applications (Gens, 2013).

The brittleness of structured geomaterials also governs their cyclic behaviour. Indeed, structured soils can undergo progressive destructuration under cyclic loading due to inelastic strain accumulation (e.g., Lefebvre & LeBoeuf, 1987; Sharma & Fahey, 2003b). Depending on the characteristics of the cyclic loading, the structure metastability can lead to abrupt failure with a rapid increase in inelastic strains when the applied stress tends to the material strength, which is reduced from its initial peak value (e.g., Ahmadi-Naghadeh et al., 2022; Ushev & Jardine, 2022). Hard soils and soft rocks are therefore known to be particularly sensitive to fatigue loading, with fatigue life (defined as the number of cycles to failure) depending on a wide range of loading parameters, including maximum and mean applied stresses, loading amplitude, frequency, waveform type and confinement pressure (e.g., Lefebvre & LeBoeuf, 1987; Ahmadi-Naghadeh et al., 2022; Ushev & Jardine, 2022; see also Cerfontaine & Collin, 2018, for a comprehensive review of rock fatigue response).

Typical geotechnical areas involving structured geomaterials include slope stability problems (e.g., Potts et al., 1997; Mesri & Shahien, 2003), dams and embankments (e.g., Potts et al., 1990; Chen et al., 1992), and deep excavations, particularly where the formation is considered a potential host for radioactive waste disposal (e.g., Bernier et al., 2007; Lisjak et al., 2014). Instead, the fatigue behaviour of this class of materials has mainly been investigated in relation to the cyclic response of foundations subjected to seismic, wind or wave loading, as required for the design of offshore and onshore foundations (e.g., Ahmadi-Naghadeh et al., 2022; Ushev & Jardine, 2022).

However, the mechanical response of structured clays is also of particular importance in reservoir geomechanics. Hydrocarbon reservoirs consist of a porous host formation surrounded by a low permeability

caprock which prevents the migration of hydrocarbons. Such caprocks are typically either evaporites or, in many cases, sedimentary argillaceous rocks with varying degrees of bonding. The mechanical effects of hydrocarbon production have been shown to cause significant compaction of the reservoir, resulting in surface subsidence and reduction in the deviatoric stress state of the overlying caprock formation (e.g. Hettema et al., 2000), whereas gas injection leads to a gradual expansion of the host formation, implying an increase in the deviatoric stress of the overburden (Lavrov, 2016). In recent years, the mechanical response of caprock materials has also attracted attention in relation to other energy-related applications, such as temporary storage of natural gas (e.g. Teatini et al., 2011) and seasonal regulation of hydrogen production from renewable energy sources (e.g. Heinemann et al., 2018). In such applications, depleted reservoirs are used as storage sites due to their large capacities and global availability. Unlike conventional oil and gas applications, underground gas storage results in cyclic stress paths in the caprock driven by reservoir deformation, which can lead to degradation of the material structure, potentially compromising its sealing integrity (e.g. Jeanne et al., 2020). It is therefore of paramount importance to assess potential fatigue-related risks associated with underground gas storage. The detrimental effects of fatigue loading have already been widely recognised in the context of gas storage in salt caverns (e.g. He et al., 2019). In contrast, the fatigue behaviour of soft clayey rocks from high depths has not yet been investigated in depth.

This paper presents an experimental investigation of the undrained monotonic and cyclic response of a deep structured clay, constituting a typical caprock formation. The fatigue behaviour of the material was studied in relation to the influence of the loading period T and to the combined effects of the parameters defining the imposed cyclic deviatoric stress history, namely: the maximum deviatoric stress q_{max}, the mean deviatoric stress q_{mean}, and the loading amplitude A. The tests were performed at high confining pressures in accordance with the expected in situ stress state. In addition, special attention was paid to the analysis of the time dependence of the mechanical response, since underground gas storage operations are usually associated with very slow processes, which are not compatible with the usual test times.

2 Methodology

2.1 Material properties and sampling procedures

The studied material is a Plio-Pleistocene stiff clay cored from a deep formation from the Po valley in Italy known as Santerno clay (e.g., Benetatos et al., 2023). It was selected as it represents a typical caprock of a hydrocarbon reservoir. Intact samples were retrieved from a depth of approximately 1150 m and then immediately sealed to preserve their undisturbed state. Samples disturbance was investigated by Ciancimino et

al. (2024) using initial suction measurements. Initial suction was found to be only slightly higher than that theoretically expected under ideal undisturbed coring conditions, suggesting that very minor drying occurred during coring and storage. In addition, laboratory measurements of shear and compressional wave velocities, taken at a stress state consistent with that in situ, were in excellent agreement with the results from borehole sonic logs. These observations suggest that the samples can be considered representative of the in-situ material response, as no significant change in their structure had occurred during coring, storage and saturation stages.

Santerno clay can be classified as a clay with silt (clay and silt fractions equal to 50% and 49%, respectively) with liquid limit w_L = 43.5% and plastic limit w_P = 25.3% (plasticity index PI = 18.2%). From a mineralogical point of view, it is composed of about 36.3% of clay minerals, with Illite and Kaolinite being the dominant ones. The percentage of carbonates is about 38.8%, with Calcite at 28.1% and Dolomite at 10.7% (data after Ciancimino et al., 2024). Such abundance of carbonate minerals suggests the presence of a post-sedimentation structure which may include diagenetic carbonate bonding.

The role of structure was investigated through high-pressure oedometer tests carried out on both intact and reconstituted specimens with a height of 20 mm and a diameter of 25.2 mm. Three tests were carried out on natural Santerno clay and one on reconstituted material. The reconstituted specimen was prepared by one-dimensional compaction of a thoroughly mixed slurry with a water content $w = 1.5 w_L$. This procedure ensures that the mechanical properties of the specimen are completely independent of its natural state and can therefore be identified as intrinsic properties (Burland, 1990).

The results are shown in Figure 1 in terms of void ratio e as a function of σ'_v. The oedometer test carried out on reconstituted material shows a relatively stiff response to reloading up to the pre-consolidation stress (equal to 9 MPa) applied during reconstitution. Beyond this value, the material tends towards normally consolidated conditions, so that the compression curve can be interpreted as the intrinsic compression line, whose estimate is shown in the graph. On the contrary, intact Santerno clay shows a very stiff behaviour with only a slight hint of curvature for σ'_v larger than 10 MPa. No clear yielding can be detected, suggesting a yield stress value σ'_{vy} larger than the maximum stress σ'_v = 58 MPa achieved. The in-situ stress state was reconstructed from direct borehole measurements together with analysis of log data and was found to be σ'_{v0} = 12.3 MPa and σ'_{h0} = 6 MPa. These values would result in a yield stress ratio YSR > 4.5 (being $YSR = \sigma'_{vy} / \sigma'_{v0}$, after Burland, 1990). Such a large YSR cannot be considered as the consequence of erosion or other tectonic processes, nor to creep (e.g. Leonards & Altschaeffl, 1964), suggesting a significant material structure. This hypothesis is further supported by the observation that the oedometric curve of the natural material clearly crosses that of the reconstituted specimen. Indeed, as will be shown in section 3.1, the fragile material response

147 suggests a relevant post-sedimentation structure, since as noted by Cotecchia and Chandler (2000), diagenetic
148 effects are expected to play a significant role for natural materials at large depths, where both temperature and
149 pressure are high.

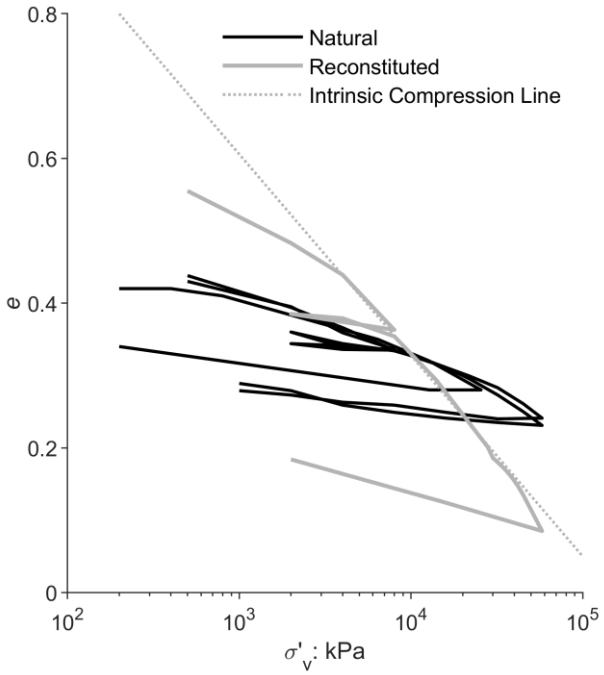

150
151 Figure 1: Results of high-pressure oedometer tests performed on natural and reconstituted specimens of Santerno clay

152 ## 2.2 Experimental procedures and testing programme

153 The mechanical response of natural Santerno clay was investigated by means of undrained monotonic and
154 cyclic triaxial tests performed on either the medium- or the high-pressure triaxial apparatus (MPTA or HPTA,
155 respectively) of the Politecnico di Torino (see also Barla et al., 2010). Specimens of 100 mm height and 50 mm
156 diameter were tested in the HPTA, while tests performed on the MPTA used 76 mm height and 38 mm diameter
157 specimens. A pair of vertical linear displacement transducers mounted diametrically opposite on the central part
158 of the specimens measured local axial displacements. Global measurements were also taken using external
159 transducers calibrated to remove spurious displacements due to the deformability of the apparatus. When not
160 clearly specified in the text, reference is made to axial strains from external transducers. This was done because
161 divergent local axial strains were measured upon shearing due to the formation of a well-defined shear band
162 within the specimens. However, external and local measurements prior to failure were found to be almost
163 identical (see Figure 4).

164 The test protocol consisted of the classic three phases of triaxial testing: saturation, consolidation, and
165 shear. The saturation procedure included both a flushing step and a back pressure sequence to ensure complete
166 saturation of the specimen and the entire apparatus, with final Skempton's (1954) B-values larger than 0.97.

This phase was carried out under an effective confining stress of about 400 kPa, in order to avoid excessive disturbance effects induced by swelling of the specimens. As mentioned above, the absence of significant destructuration is also supported by the alignment of laboratory and in situ measurements of shear and compressional wave velocities at the end of the consolidation phase. Consolidation was carried out up to the expected lithostatic stress state, namely: p'_0 = 8.1 MPa and q_0 = 6.3 MPa. Full drainage through the external surfaces was achieved by placing filter paper strips all around the boundaries of the specimen. The stress state was increased in a sufficiently large time to ensure practically drained conditions. Shear was then applied in compression under undrained conditions. Pore water pressure build-up was measured using external transducers connected to the top and bottom bases of the specimens. No significant differences were observed between the two measurements during triaxial testing. Further details about the experimental procedures can be found in Ciancimino et al. (2024).

A summary of the experimental program is presented in Table 1. Three specimens were monotonically sheared under strain control imposing different axial strain rates $\dot{\varepsilon}_{ax}$, namely; 0.0005 %/min, 0.01 %/min, and 0.5%/min (data after Ciancimino et al., 2024). The strain rate of 0.01 %/min corresponds to the reference value computed according to ASTM D4767-11 (2020) standard. The other two values were chosen to show the importance of time dependence in the mechanical response of the Santerno clay and to provide a basis for interpretation of the cyclic tests. These were carried out under stress-control by imposing a sinusoidal deviatoric load. A schematic representation of the loading protocol is shown in Figure 2. Under undrained conditions, the deviatoric stress was firstly increased from q_0 to the mean value q_{mean} around which the cyclic loading was applied. The load was then held constant until the axial strain and pore pressure were practically stable. Finally, the sinusoidal history was applied according to a certain amplitude A up to a maximum deviator $q_{max} = q_{mean} + A$ and down to a minimum one $q_{min} = q_{mean} - A$. The cycles were applied with a period T of either 5 min or 250 min. Similarly to Ushev and Jardine (2022), the first value was chosen as a good compromise between accuracy of load control, reliability of pore pressure measurements and feasibility of the testing times. Instead, the longer period was chosen to investigate the time dependence of the cyclic material response.

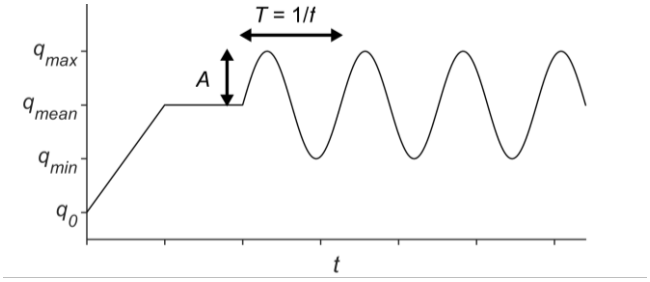

Figure 2: Loading protocol at shear for cyclic triaxial tests

Table 1: Summary of the anisotropically consolidated undrained triaxial tests

ID	Type	Apparatus	$\dot{\varepsilon}_{ax}$ or $\bar{\dot{\varepsilon}}_{ax}$: %/min	q_{max}: MPa	A: MPa	q_{mean}: MPa	T: min	N_f	Reference
M-TX 01	Monotonic	HPTA	0.01	-	-	-	-	-	Ciancimino et al. (2024)
M-TX 02	Monotonic	HPTA	0.5	-	-	-	-	-	Ciancimino et al. (2024)
M-TX 03	Monotonic	MPTA	0.0005	-	-	-	-	-	Ciancimino et al. (2024)
C-TX 01	Cyclic	MPTA	0.18	13	3.25	9.75	5	18	Ciancimino et al. (2024)
C-TX 02	Cyclic	HPTA	0.24	11.8	5.45	6.35	5	> 4635	This study
C-TX 03	Cyclic	MPTA	0.004	11.9	5.2	6.7	250	> 238	This study
C-TX 04	Cyclic	MPTA	0.004	13	5.25	7.75	250	7	This study
C-TX 05	Cyclic	MPTA	0.19	13	5.25	7.75	5	60	This study
C-TX 06	Cyclic	HPTA	0.33	13.5	5.95	7.55	5	13	This study
C-TX 07	Cyclic	MPTA	0.27	12.5	5.25	7.25	5	1146	This study
C-TX 08	Cyclic	MPTA	0.10	12.5	3.25	9.25	5	77	This study
C-TX 09	Cyclic	MPTA	0.16	12.5	4.25	8.25	5	173	This study

The loading characteristics are presented in Table 1, along with the number of cycles to failure N_f and the average axial strain rate applied during cyclic loading $\bar{\dot{\varepsilon}}_{ax,c}$. It should be noted that under cyclic, stress-controlled conditions, failure occurs as a rapid accumulation of axial strains, tending towards extremely large values. As the maximum strain rate applicable to the specimens is limited by the maximum axial displacement velocity of the apparatus, this often results in a reduction in the maximum applied deviatoric stress as failure approaches (see also Figure 5a, presented in the following). To avoid any possible ambiguity in the definition of N_f, failure was considered to have occurred when the apparatus was no longer able to apply a deviatoric stress equal to 95% of q_{max}. $\bar{\dot{\varepsilon}}_{ax,c}$ was computed by referring to the average axial strain applied during one quarter of cyclic loading $\bar{\varepsilon}_{ax,c}$ as:

$$\bar{\dot{\varepsilon}}_{ax,c} = \frac{4\bar{\varepsilon}_{ax,c}}{T} \quad (1)$$

Such a value is only indicative of the order of magnitude of the resulting strain rate, as the actual rate changed continuously during the stress-controlled cyclic tests. However, it can be used as a reference to compare monotonic and cyclic tests in a consistent manner. For the tests carried out at T = 5 min, the resulting $\bar{\dot{\varepsilon}}_{ax,c}$ values are reasonably close to the faster monotonic test (i.e. with $\dot{\varepsilon}_{ax}$ = 0.5 %/min). Conversely, the cyclic loads with T = 250 min yield $\bar{\dot{\varepsilon}}_{ax,c}$ values which are closer to the monotonic test carried out at $\dot{\varepsilon}_{ax}$ = 0.01 %/min.

3 Stress-strain response and stress paths

3.1 Undrained monotonic behaviour

The role of the material structure is clear from the stress-strain $q-\varepsilon_{ax}$ curves and the stress-paths $q-p'$ resulting from the undrained monotonic tests shown in Figure 3 (experimental data after Ciancimino et al., 2024). The response is quite stiff up to the peak shear strength. The deviatoric stress then suddenly decreases at the onset of brittle failure and shows a pronounced softening branch up to the post-rupture strength (Figure 3a). As suggested by Burland (1990), this reduction is mainly associated with interparticle debonding. It can therefore be inferred that in the intact Santerno clay is present a metastable structure which suddenly degrades after yielding, leading to the development of a sharp shear band (see also Ciancimino et al., 2024). Subsequently, a further gradual reduction towards stable conditions is observed. The onset of shear banding can be detected by comparing local and global axial strain measurements, $\varepsilon_{ax,l}$ and $\varepsilon_{ax,g}$ respectively, as shown in Figure 4 for tests M-TX 01 and M-TX 02. Local and external measurements are practically equivalent up to the peak deviatoric stress, while they start to diverge significantly in the softening branch (i.e. for $\varepsilon_{ax,g}$ larger than 1.5% and 2% respectively for tests M-TX 01 and M-TX 02).

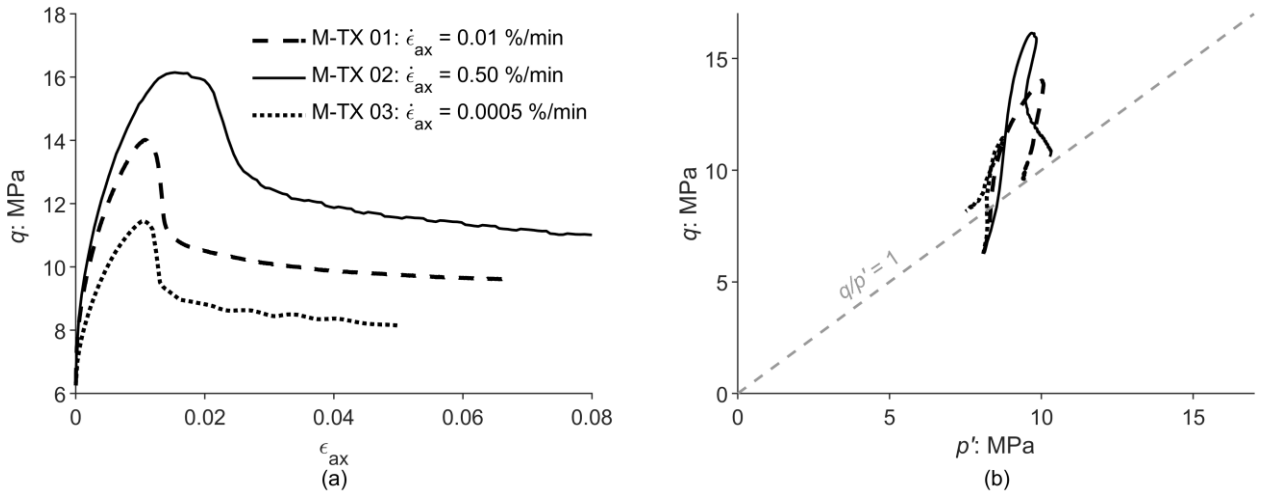

Figure 3: Undrained monotonic response under different axial strain rates: (a) stress-strain behaviour; (b) effective stress-paths (data after Ciancimino et al., 2024)

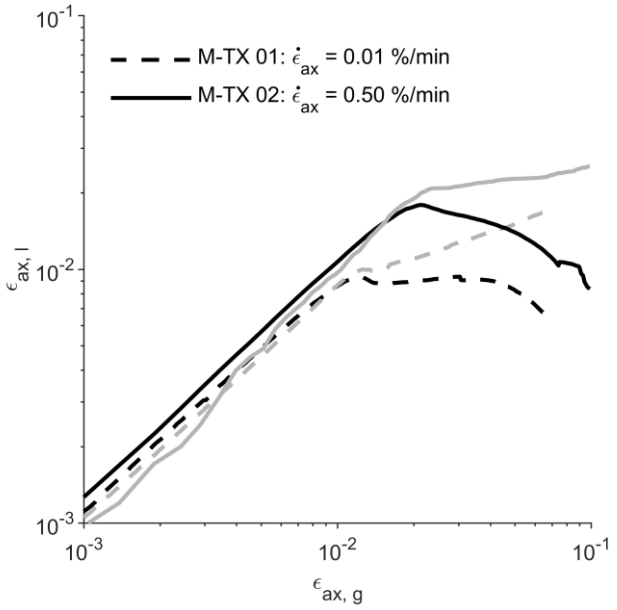

Figure 4: Comparison between local and global axial strain measurements during monotonic shear; black and grey lines refer to two different local measurements taken during the test

The peak strength strongly depends on $\dot{\varepsilon}_{ax}$. By observing the effective stress-paths (Figure 3b), each test appears to be associated with a different stress obliquity at failure. Conversely, the stress-obliquity q / p'=1 at critical state does not appear to be affected by $\dot{\varepsilon}_{ax}$. Similar observations have been reported, for example, by Vaid and Campanella (1977) for overconsolidated Leda clay, by Tavenas et al. (1978) for overconsolidated Saint-Alban clay, and by Lefebvre and LeBoeuf (1987) for structured Grande-Baleine clay. Time-dependency appears therefore to play an important role in the mechanical response of Santerno clay, and on it its peak strength envelope enlarged by the material structure.

3.2 Undrained cyclic behaviour

To analyse the distinctive features of the cyclic response of Santerno clay, test C-TX 06 is taken as an example. The results are shown in Figure 5 in terms of $q-\varepsilon_{ax}$ curves, excess pore water pressure Δu_w build-up, and $q-p'$ paths. During the first cycle, the specimen accumulates significant inelastic ε_{ax} (Figure 5a). Subsequently, the response tends to stabilize, and a smaller accumulation is observed for each cycle. Acceleration of the degradation process with increasing accumulation of inelastic strains with each cycle occurs at the 10th cycle. Similar to what was observed for monotonic conditions, this acceleration can be related to the onset of shear banding and therefore to the rapid degradation of the metastable structure associated with interparticle bonding. This hypothesis is supported by the comparison between $\varepsilon_{ax,l}$ and $\varepsilon_{ax,g}$, shown in Figure 6 as a function of the number of cycles N. The measurements begin to diverge at around the 10th cycle, while they completely diverge at the 13th cycle, which is assumed as the fatigue life N_f. Initially, no significant pore water pressure accumulation is observed from cycle to cycle (Figure 5b), resulting in a fairly stable cyclic stress

path (Figure 5c). As the specimen approaches failure, there is a progressive decrease in the excess pore water pressure, which is greater as the shear band develops, shifting the cyclic effective stress path to the right. Such a trend is consistent with the monotonic $q - p'$ paths reported in Figure 3b, which tend to the right as the peak shear strength is approached. Figure 5c also shows the monotonic peak strength envelope proposed by Ciancimino et al. (2024) for the Santerno clay when sheared at a constant $\dot{\varepsilon}_{ax} = 0.5$ %/min. This test was chosen because its $\dot{\varepsilon}_{ax}$ is somewhat consistent with the average value $\overline{\dot{\varepsilon}}_{ax,c} = 0.33$%/min obtained in the cyclic test. Cyclic failure occurs at the 13th cycle, well below the peak strength envelope. Under cyclic stress-controlled loading, the material accumulates inelastic axial strains, progressively degrading its structure and yielding to the onset of the shear band. As the maximum deviatoric stress q_{max} approaches the material strength (reduced from its initial value), fragile failure occurs.

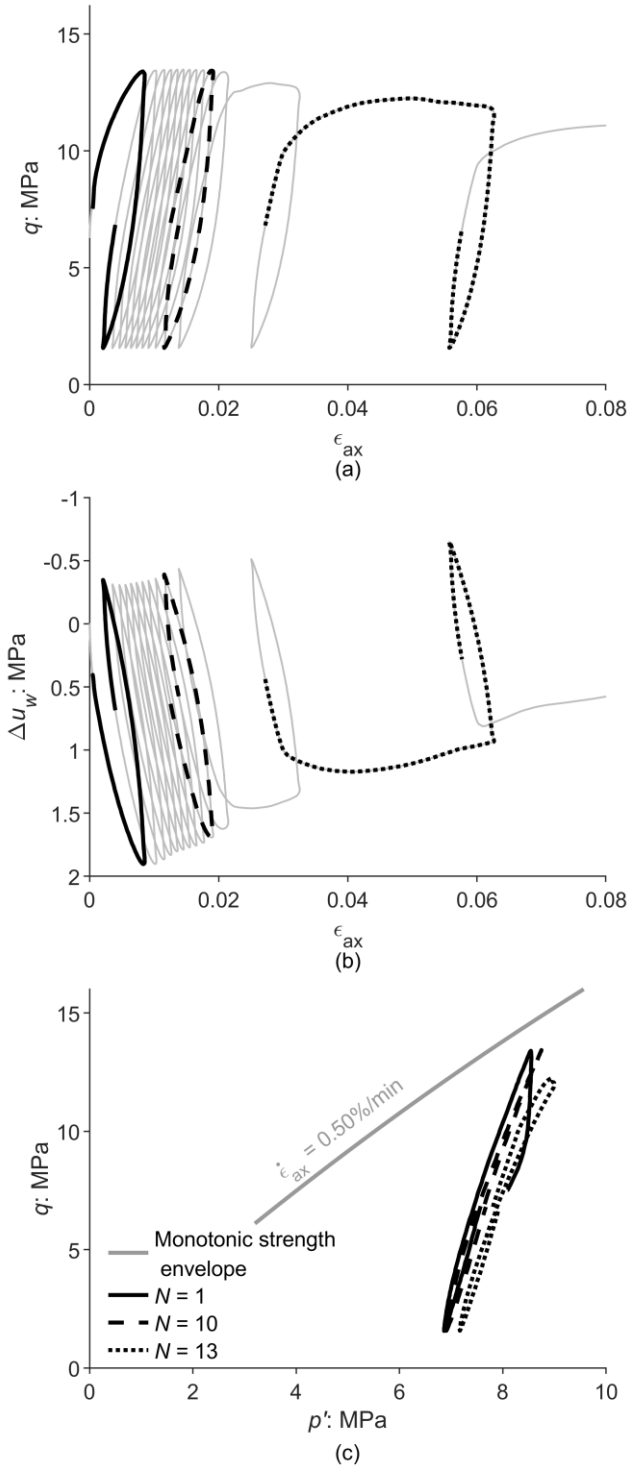

Figure 5: Undrained cyclic response (test C-TX 06, T = 5 min): (a) stress-strain behaviour; (b) pore water pressure build-up; (c) effective stress-path compared to the strength envelope suggested by Ciancimino et al. (2024) for an axial strain rate of 0.5 %/min

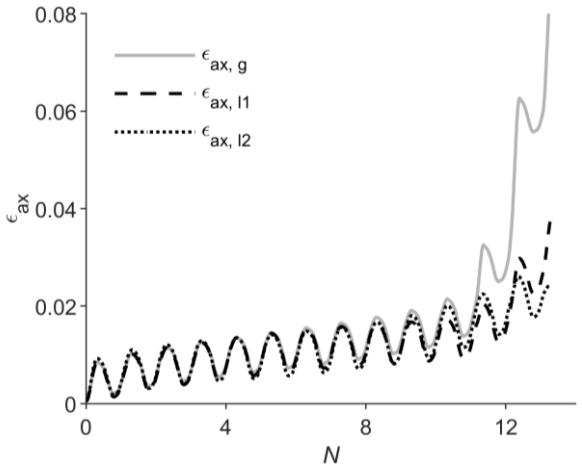

Figure 6: Comparison between local and global axial strain measurements during cyclic loading

The role of the metastable structure under cyclic loading is clear from the above discussion. To illustrate the relevance of the second aspect highlighted under monotonic conditions, i.e. the time-dependency, the results of two tests carried out at different T, 5 min and 250 min for tests C-TX 06 and C-TX 04 respectively, are compared with the monotonic curves in Figure 7. The results are presented in terms of stress obliquity q / p' with ε_{ax} (Figure 7a and Figure 7b) to normalise for possible Δu_w accumulation. Reference is made to two different monotonic curves to match the $\bar{\dot{\varepsilon}}_{ax,c}$ with the $\dot{\varepsilon}_{ax}$ applied under strain control. Additionally, Figure 7c and Figure 7d compare the actual strain rates applied during the cyclic tests with those imposed in the monotonic tests. For both cyclic tests, the $\dot{\varepsilon}_{ax}$ resulting from the stress-controlled loading approaches that imposed in the monotonic tests when the cyclic deviatoric stress is close to q_{max}. Under this condition, the monotonic curves serve as a sort of envelope for the cyclic response (Figure 7a and Figure 7b). When the permanent ε_{ax} accumulation is such that the cyclic responses approach the monotonic curves, failure occurs. Consequently, $\dot{\varepsilon}_{ax}$ rapidly increases and the cyclic stress-strain response can therefore "cross" the monotonic envelope which now refers to a smaller strain-rate value with respect to the actual cyclic one.

A similar dependence has already been observed, for example, by Lefebvre and LeBoeuf (1987) on sensitive clays retrieved at shallow depths. However, no experimental results have been reported on highly structured clays from large depths. The time dependence of the mechanical response and its relevance to the structural degradation process is a peculiar aspect of material behaviour and it is expected to govern its response to fatigue loading.

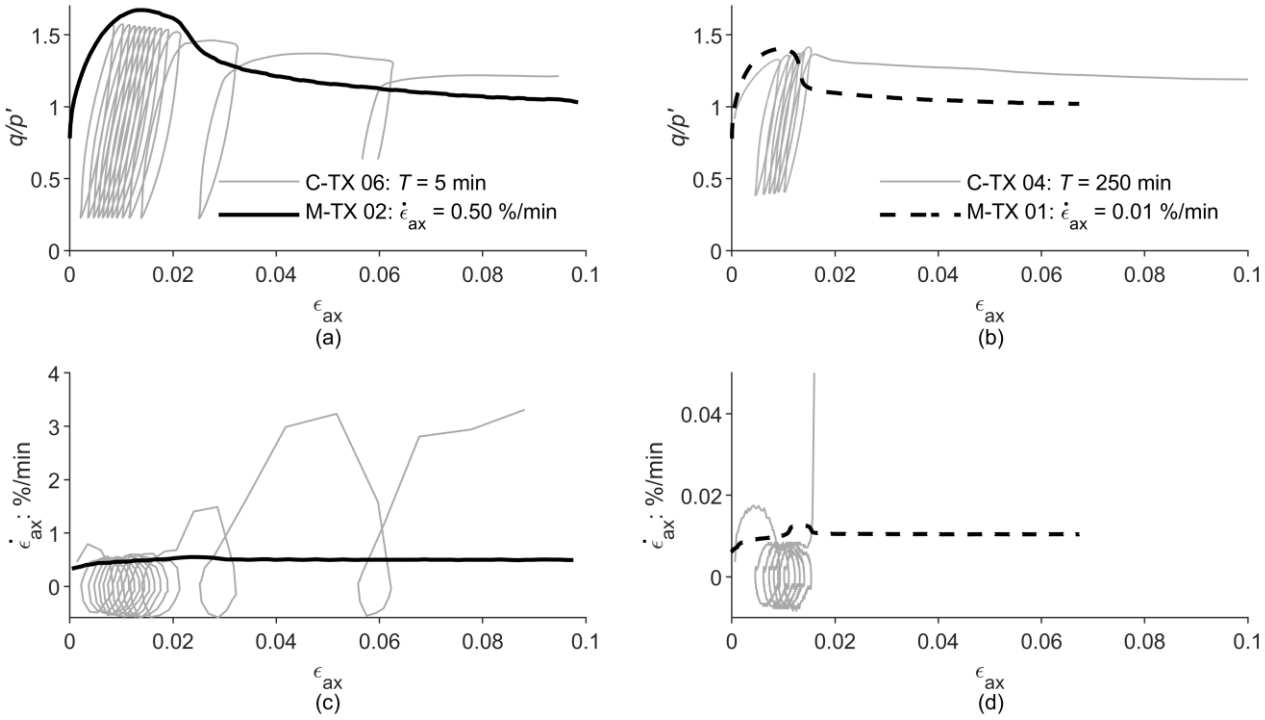

Figure 7: Comparison between monotonic and cyclic responses observed in tests performed at consistent strain rates: (a-b) stress ratio vs axial strain; (c-d) axial strain rate vs axial strain

4 Fatigue response

The results of the cyclic tests can be summarised in three underground gas storage scenarios: *(i)* different storage regulations, e.g., daily or seasonal variations, can be studied by imposing the same deviatoric stress history but with different periods T ; *(ii)* the maximum amount of gas stored can be somehow related to the maximum deviatoric stress q_{max} imposed to the caprock formation; and *(iii)* the amplitude A can be associated with reservoir pressure declines needed to balance energy supply and demand cycles.

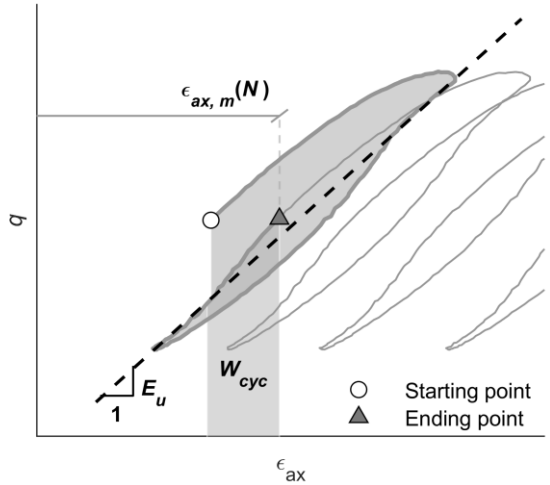

Figure 8: Definition of the cyclic parameters adopted to describe the undrained stress-strain loops

The fatigue response of Santerno clay is analysed with reference to these scenarios using a set of synthetic cyclic parameters as defined in Figure 8 for a typical stress-strain loop. The mean axial strain $\varepsilon_{ax,m}$ is the value measured at the end of a loading cycle, while the unloading secant Young's modulus E_u is used to evaluate the stiffness degradation. W_{cyc} represents the energy dissipated within the N^{th} loading cycle, calculated as:

$$W_{cyc} = \int_{\varepsilon_{ax,m}(N-1)}^{\varepsilon_{ax,m}(N)} q \cdot d\varepsilon_{ax} \tag{2}$$

Stress-strain loops are not closed due to the accumulation of inelastic strains, resulting in significant energy dissipation as shown by the dark grey shaded area represented in Figure 8. W_{cyc} can therefore be considered representative of the damage process, as often assumed in rock fatigue studies (e.g., Cerfontaine & Collin, 2018). In addition, information on the pore water pressure build-up is presented by the average $\Delta u_{w,m}$ measured at the end of each load cycle.

4.1 Role of loading period

The same deviatoric history applied with different periods implies significantly different resulting strain rates and total test durations. By virtue of the role played by the time dependence of the mechanical response, progressive destructuration occurs at increasing cyclic rates as T increases. Figure 9 compares the cyclic parameters for two tests performed with the same deviatoric stress values but different T, namely tests C-TX 04 and C-TX 05 corresponding to T = 250 min and 5 min respectively.

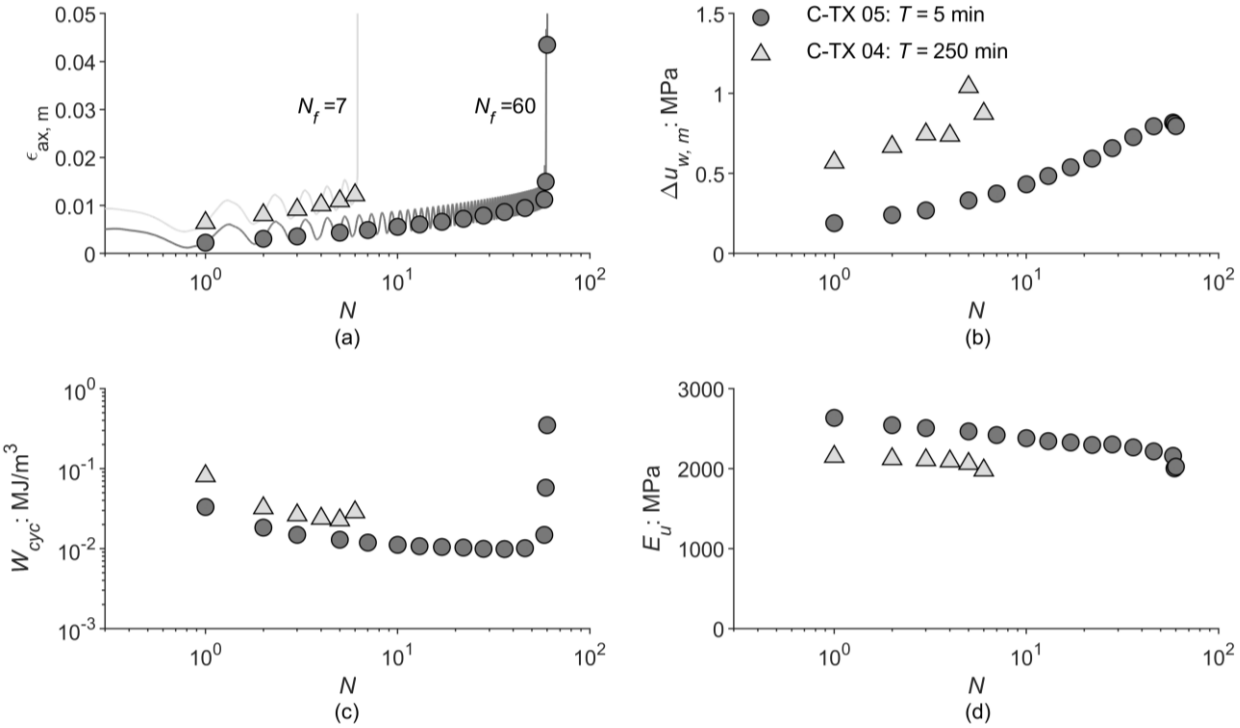

Figure 9: Influence of the period on the evolution of the material response with loading cycles: (a) mean axial strain; (b) mean excess pore water pressure; (c) cyclic strain energy; d) unloading secant Young's modulus

By observing the evolution of $\varepsilon_{ax,m}$, it is possible to identify the typical behaviour of cemented materials subjected to cyclic loadings with q_{max} close to the monotonic strength (Figure 9a). The initial "deceleration" and "stabilisation" phases of axial strain accumulation, typical of the fatigue behaviour of brittle materials (e.g., Fuenkajorn & Phueakphum, 2010) are quite short, especially in the case of test C-TX 04. Failure occurs at the 7th and 60th cycle for tests C-TX 04 and C-TX 05 respectively, where a rapid increase in the permanent strains indicates the development of the shear band, associated with the "acceleration" phase. Although the same history was applied in terms of deviatoric stress values, the influence of the loading period T is such that an almost tenfold increase in the fatigue life N_f is observed in the test characterised by a shorter T.

The onset of cyclic failure can also be identified in Figure 9c, which shows the evolution of W_{cyc}. For both tests, a sudden increase in W_{cyc} is observed when approaching failure. However, test C-TX 04 shows a larger energy dissipation even in the first cycles, reflecting the larger accumulation of inelastic strains. Test C-TX 04 also shows a faster increase in $\Delta u_{w,m}$ (Figure 9b), reaching a value of about 1 MPa in 6 cycles consistent with the Δu_w measured in test M-TX 01 just before failure. Almost the same value is reached in 60 cycles in test C-TX 05. When approaching failure, both specimens show a stabilisation or even a decrease of $\Delta u_{w,m}$. Such a response is typically associated with the development of the shear band (Burland, 1990).

The secant modulus E_u shows a progressive and almost linear (on a semilogarithmic scale) decrease with N (Figure 9d). Such a decrease somewhat reflects cyclic destructuration, as has been observed for other cemented materials (e.g., Sharma & Fahey, 2003a; Ushev & Jardine, 2022). Comparing the results of the two tests, E_u appears strongly influenced by T. Although the value of A was the same for both tests, their nonlinear response was indeed significantly different, with a greater deformability for test C-TX 04, which was conducted at a larger T.

4.2 Combined effect of maximum deviatoric stress and mean deviatoric stress

The maximum imposed deviatoric stress q_{max} is generally considered to be the most influential factor in the fatigue life of structured materials. Its relevance is analysed in Figure 10 by comparing tests C-TX 01 and C-TX 08, carried out imposing the same $A = 3.25$ MPa and $T = 5$ min but different q_{max} equal to 13 MPa and 12.5 MPa respectively. However, it should be noted that tests carried out imposing the same A but different q_{max} are necessarily characterized also by different $q_{mean} = q_{max} - A$. Therefore, the results of this set of tests should be interpreted as the combined effect of both q_{max} and q_{mean}, rather than as the influence of just one parameter.

The evolution of $\varepsilon_{ax,m}$ shows a more rapid increase from the first cycles in test C-TX 01 performed at larger q_{max}, and in turn q_{mean}, leading to specimen failure after 18 cycles (Figure 10a). In contrast, 77 cycles are required to reach the fatigue life in test C-TX 08. At the same time, $\Delta u_{w,m}$ is slightly higher in test C-TX 01, likely because of the higher q_{mean} imposed (Figure 10b). In both tests, a decreasing trend of $\Delta u_{w,m}$ is observed when approaching failure, suggesting the development of the shear band.

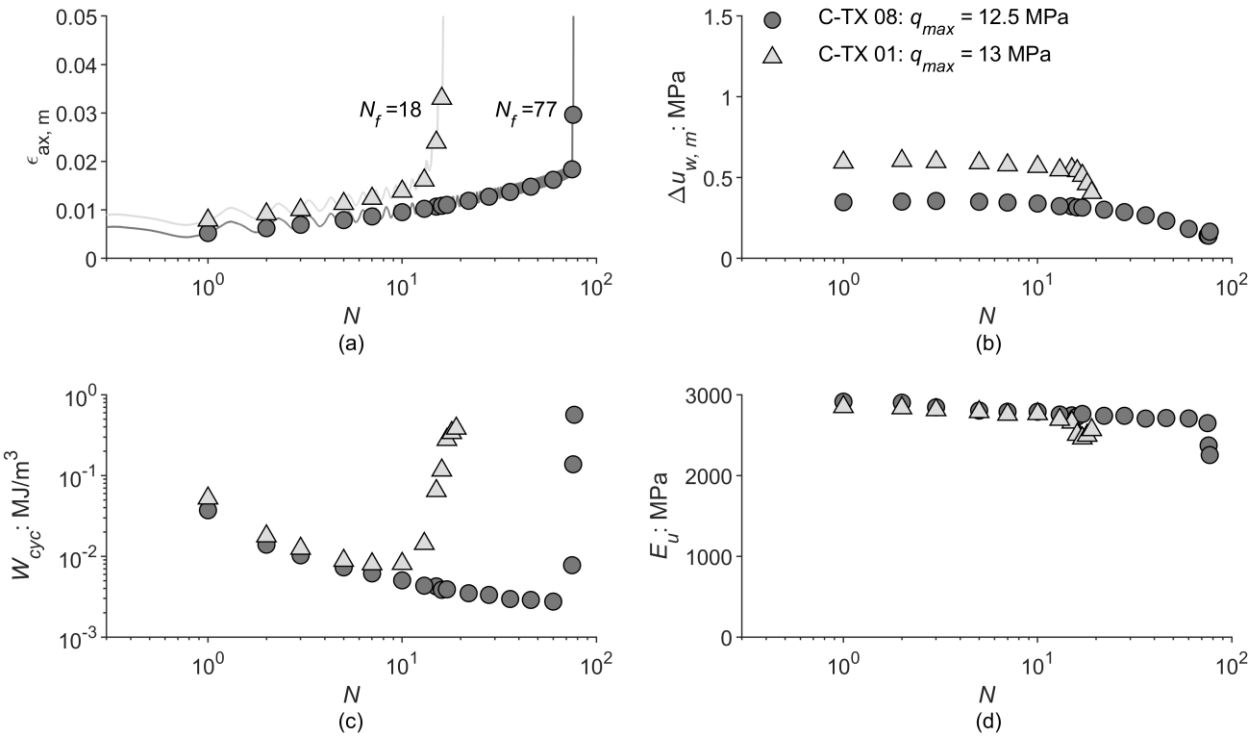

Figure 10: Influence of the maximum (and mean) deviatoric stress on the evolution of the material response with loading cycles: (a) mean axial strain; (b) mean excess pore water pressure; (c) cyclic strain energy; d) unloading secant Young's modulus

The measured values of E_u and W_{cyc} are practically equivalent in the two tests before approaching failure. These quantities appear being characteristic of the material response within a single load cycle and are predominantly defined by the value of A, which is 3.25 MPa in both tests. A rapid increase in W_{cyc} can be detected close to the failure condition (Figure 10c). On the other hand, E_u shows a modest, and again almost linear, reduction with N, with a slightly more marked decrease only in the last few cycles (Figure 10d).

To analyse the influence of q_{max} on N_f, reference can be made to Figure 11 which shows the results of tests performed at almost the same amplitude (i.e. $A \approx 5.25$ MPa - 5.45 MPa), except for test C-TX 06, for which a slightly larger value (i.e. $A = 5.9$ MPa) was imposed. Tests C-TX 02 and C-TX 03 were interrupted before reaching failure due to their excessive duration; the results are therefore plotted for comparison purposes

only. Looking at the tests carried out with T = 5 min, the N_f - q_{max} data appear to be well approximated by a linear relationship (on a semi-logarithmic scale). Based on this line, it is reasonable to assume that test C-TX 02 could have led to failure of the specimen, but at the cost of a very high number of cycles applied, which was not compatible with the testing times.

The results presented in Figure 11 show the relevance of q_{max} on N_f. However, as previously mentioned, this relevance should be interpreted as the combined effect of q_{max} and q_{mean}, which cannot be decoupled. As will be better clarified in more detail below, an increase in q_{mean} can lead a significant reduction in N_f. Therefore, it is reasonable to infer that if test C-TX 06 had been carried out at the same amplitude as the other tests presented in Figure 11, the alignment with the represented line would likely have been even better. This is because it would have been associated with a higher q_{mean} and, in turn, a smaller N_f.

The comparison between tests performed at approximately the same q_{max} but different T suggests that an increase in the imposed rate of deformation leads to a significant increase of the fatigue life. Such a difference is particularly significant for the tests shown here and cannot be neglected given the very long timescales associated with the phenomena under consideration.

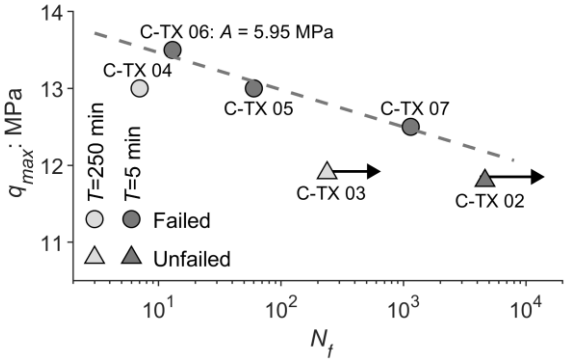

Figure 11: Influence of the maximum (and mean) deviatoric stress on the fatigue life of the material (tests performed with $A \approx$ 5.25 - 5.9 MPa).

4.3 Combined effect of loading amplitude and mean deviatoric stress

Sinusoidal deviatoric loadings characterized by the same q_{max} but different A are also characterized by different q_{mean}. Figure 12 shows the comparison in terms of stress-strain response between tests C-TX 08, C-TX 09 and C-TX 07 carried out at the same T = 5 min and q_{max} = 12.5 MPa but different A, equal to 3.25 MPa, 4.25 MPa and 5.25 MPa respectively. The three cyclic histories result in similar $\bar{\varepsilon}_{ax,c}$ (see also Table 1) and are in good agreement with the monotonic envelope obtained at a consistent strain rate. However, an increase in A appears to produce an increase in N_f as a consequence of smaller accumulation of permanent strains in each cycle and of the larger ε_{ax} required to reach brittle failure.

The comparison is proposed in Figure 13 in terms of cyclic parameters. As A decreases, a faster accumulation of $\varepsilon_{ax,m}$ is observed (Figure 13a), resulting in a lower N_f, which is equal to 77, 173 and 1146 respectively for tests C-TX 08, C-TX 09 and C-TX 07. Consistently, a slower $\Delta u_{w,m}$ accumulation is observed for tests with a larger A and therefore lower q_{mean} (Figure 13b). On the contrary, the parameters related to the material response within a load cycle appear to be negatively affected by an increase in A. Larger nonlinearity is observed with increasing A, which therefore results in lower initial values of E_u (Figure 13d). A faster degradation of E_u with N is also visible before approaching failure, as highlighted by the slopes of the data. At the same time, a larger amount of W_{cyc} is dissipated by specimens subjected to larger A cycles (Figure 13d).

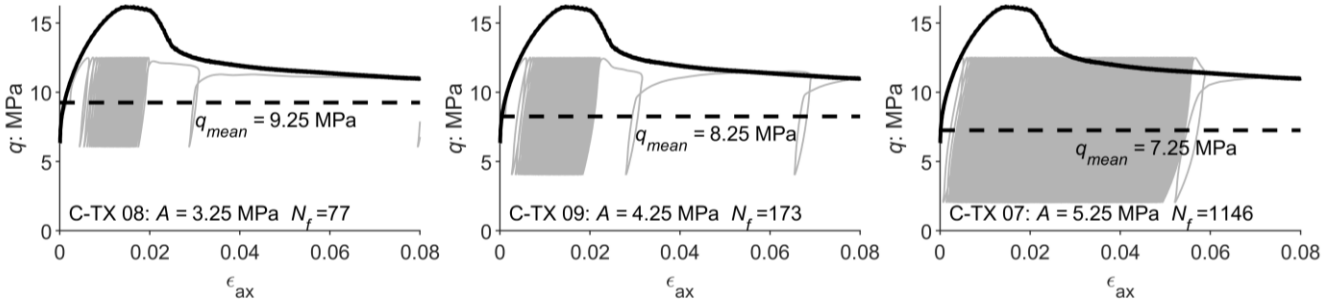

Figure 12: Cyclic stress-strain response of specimens sheared adopting the same maximum deviatoric stress and period but different loading amplitude; cyclic data compared to the monotonic curve obtained at an axial strain-rate of 0.5 %/min

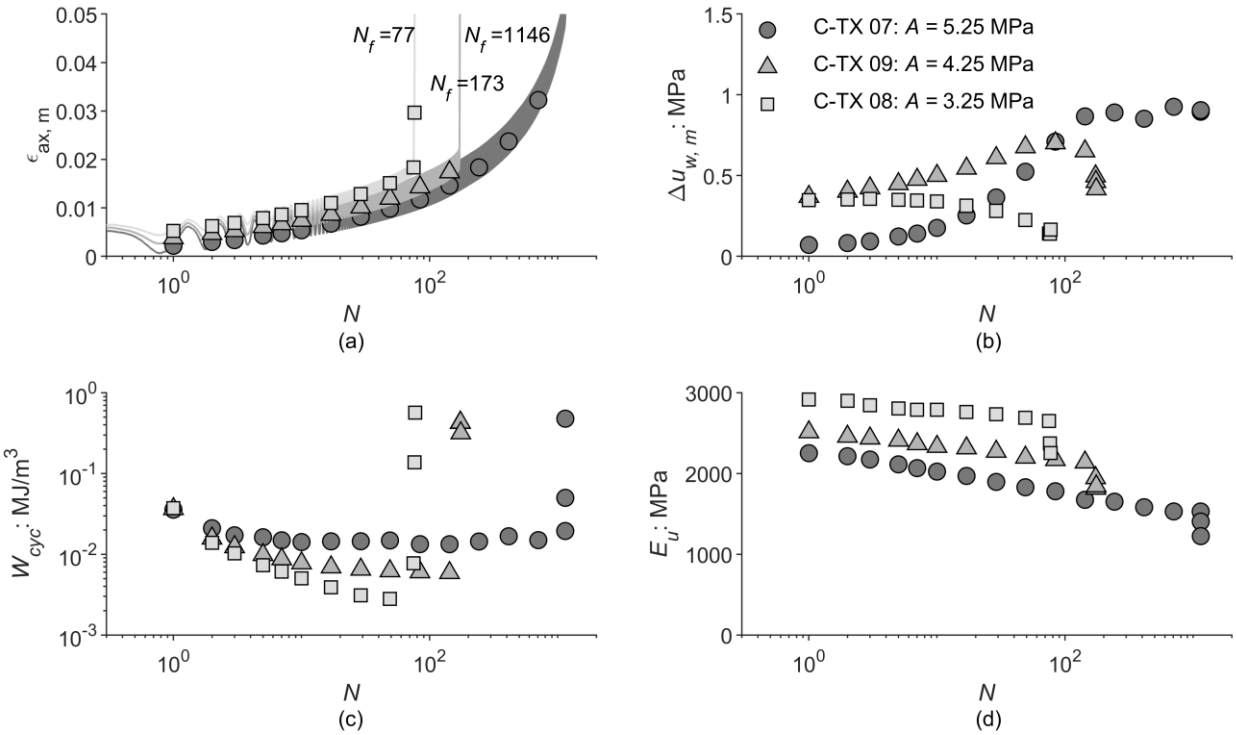

Figure 13: Influence of the amplitude (and the mean deviatoric stress) on the evolution of the material response with loading cycles: (a) mean axial strain; (b) mean excess pore water pressure; (c) cyclic strain energy; d) unloading secant Young's modulus

5 Discussion

The cyclic tests draw a fairly clear picture of the response of intact Santerno clay to fatigue loading. Its mechanical behaviour strongly depends on its structure, which degrades progressively with the applied load cycles. The rate at which this degradation occurs is certainly influenced by the loading period. As T increases, the applied strain rate decreases and so also the corresponding monotonic strength. Consequently, the fatigue life N_f of the material also decreases.

The analysis of tests carried out with the same T and A clarifies the combined effect of q_{max} and q_{mean}. As expected, N_f tends to decrease as q_{max} and, in turn, q_{mean} increase. The results of Figure 11 are in good agreement with experimental results from the literature on structured materials, which report the q_{max} as the main defining parameter of N_f (e.g., Sharma & Fahey, 2003b; Ahmadi-Naghadeh et al., 2022). This dependence appears to be approximated by a linear relationship on a semi-logarithmic scale (see Figure 11). Instead, the results of tests performed with the same q_{max} but different A show a counterintuitive response. The strength seems to degrade earlier for tests conducted at lower A. Such observation contrasts with the results of some literature studies carried out on other structured materials (see e.g. the results on chalk by Ahmadi-Naghadeh et al., 2022), where the amplitude was identified as a parameter which reduces the fatigue life.

A physical explanation for this discrepancy can be attempted introducing the dependency of N_f from A but also from q_{mean}, as shown in Figure 14 for two sets of tests characterized by the same q_{max} and T, and recalling for the role of stress state on time-dependent behaviour. Several experimental studies report the highly time-dependent behaviour of structured clays and clayrocks (e.g., Lefebvre & LeBoeuf, 1987; Al-Bazali et al., 2008; Sone & Zoback, 2014). The same aspect was also observed for the natural Santerno clay, as discussed in section 3. Under monotonic strain-controlled conditions, such a dependence is reflected in an influence of the strain rate on the peak shear strength (see Figure 3). For stress-controlled tests, this aspect results in a significant accumulation of axial strains over time, which increases with increasing deviatoric loading, as it is typically observed in creep tests (e.g., Tavenas et al., 1978). The degradation that occurs because of cyclic one-way loadings can be seen as a combination of two distinct mechanisms operating simultaneously. On the one hand, load reversals induce a progressive cyclic degradation, which is faster the larger is A, explaining the trends observed in Figure 13d for E_u. On the other hand, the application of the cyclic history takes place over a time during which a load with a mean value equal to q_{mean} is applied to the specimen. This implies the accumulation of viscous axial strains, which are typically larger the larger is q_{mean}, and which in turn induce progressive destructuration. The cyclic degradation and the viscous mechanism work together to accumulate inelastic strains, leading to strength degradation and ultimately fragile failure due to the metastability of the material.

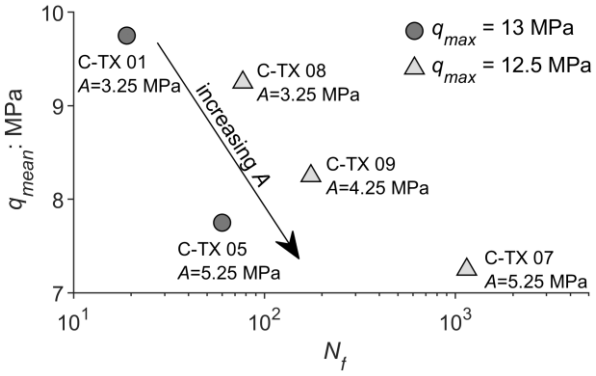

Figure 14: Influence of mean deviatoric stress and loading amplitude on the number of cycles to failure (T = 5 min)

When analysing the results of tests performed with the same q_{max} – a comparison not often reported in experimental studies in the literature – it should be considered that an increase in the value of A has a dual effect. It enhances the cyclic degradation mechanism associated with load reversal (and therefore with A), but it reduces the rate of accumulation of viscous strains (mainly governed by q_{mean}). The experimental results presented here and summarised in Figure 14 suggest that for specimens of Santerno clay subjected to one-way loadings the viscous mechanism somehow prevails. This is probably due to the rather large q_{mean} values and loading periods adopted for the cyclic histories, which increase the relevance of viscous strain accumulation.

Figure 15 illustrates the relevance of the two governing mechanisms, i.e. cyclic degradation and viscous strain accumulation, by showing the evolution of the unloading secant Young's modulus normalized to its initial value $E_u / E_{u,i}$ for three tests characterized by the same A = 5.25 MPa, but different T or q_{mean}. The tests present similar cyclic degradation of $E_u / E_{u,i}$ with N, suggesting that this aspect is predominantly driven by the loading amplitude, which is the same for all three tests. However, the fatigue life N_f is very different form test to test. An increase in T implies longer loading time and, therefore, a significant decrease in N_f, as can be seen by comparing tests C TX-05 and C TX-04. Conversely, a decrease in q_{mean} implies smaller viscous strain accumulation for each cycle, resulting in increasing N_f, as can be inferred by comparing tests C TX-05 and C TX-07.

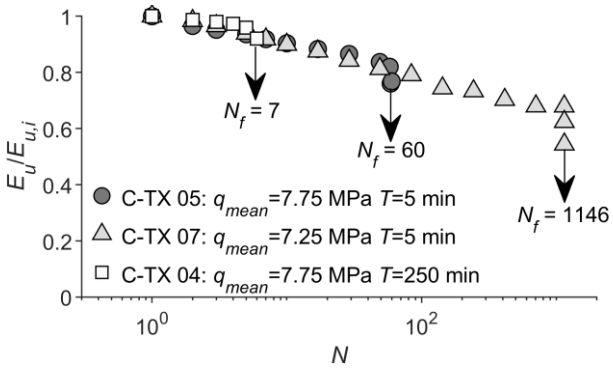

Figure 15: Cyclic evolution of the normalized unloading secant Young's modulus for tests carried out imposing the same amplitude A = 5.25 MPa

6 Conclusions

Emerging applications in energy geotechnics, such as the use of depleted hydrocarbon reservoirs as underground gas storage sites, require a more in-depth understanding of the mechanical response of structured clays. To our knowledge, no systematic experimental investigation of the triaxial response of clayey caprocks at high confinement pressure under cyclic loading has been reported. In this paper, the fatigue response of a typical deep caprock formation was investigated. Laboratory tests were carried out with particular emphasis on time-dependent effects to account for the large loading periods associated with the boundary value problem under consideration. The main conclusions of the study can be summarised as follows:

a. The first distinctive feature of the Santerno clay is the presence of a significant metastable structure. This structure was initially identified by comparing the oedometer response of intact and reconstituted specimens. Under triaxial monotonic loading, structural degradation occurs, inducing damage to interparticle bonding and changes in particle arrangement, and leading to a brittle response associated with the formation of a well-defined shear band within the specimens.
b. Structural degradation was also observed because of accumulation of inelastic strains due to fatigue loads. The initial peak strength of the intact material progressively decreases as the loading cycles are applied, leading to fragile failure. In this sense, the metastable response of the material appears to be more similar to the cyclic response of rocks than to that of non-structured clayey soils.
c. A significant time dependence of the mechanical response was observed: for monotonic strain-controlled shear as a strong influence of the applied strain rate on the peak shear strength; for the cyclic response as a dependence of the fatigue life on the loading period. Indeed, the cyclic stress-strain response can only be related to monotonic behaviour if a consistent resultant strain rate is considered.
d. Fatigue life was found to be strongly dependent on the combined effect of maximum and mean imposed deviatoric stresses. As expected, larger stresses imply larger permanent strain accumulation for each loading cycle. As a result, material degradation and failure will occur over a smaller number of cycles.
e. For one-way cyclic tests performed with the same maximum deviatoric stress, an increase in amplitude induces larger stiffness degradation due to load reversals. However, the role of the loading amplitude on the fatigue life is somewhat counterintuitive, as one would expect a lower number of cycles to failure for larger amplitudes, whereas the opposite was observed. The results obtained can be explained by considering the role of viscous strains, which are known to increase

485 with the deviatoric stress. As the amplitude increases, the mean deviatoric stress of a given cycle is
486 reduced and, therefore, the accumulated viscous strains are also reduced.

487 This study has shown the relevant role of both the structure (and its progressive degradation) and the time
488 dependence on the cyclic mechanical response of a structured clay from the Po valley. Both aspects are
489 particularly relevant for the problem under consideration, as caprock formations are frequently characterised by
490 a diagenetic structure and underground storage operations are typically associated with large loading periods. It
491 is therefore essential to use a procedure that allows the results of experimental tests to be appropriately scaled up
492 from test periods that are compatible with laboratory times to periods in the field that are significantly higher.
493 Experimental evidence suggests that these effects can be partially considered by referring to monotonic results,
494 provided that the latter are obtained by adopting a strain rate consistent with that used in cyclic tests. However,
495 it was also shown that the two distinctive features of the mechanical response interact, since the strain
496 accumulation due to the persistence of the applied load also induces structural degradation, which has a
497 significant effect on the fatigue life.

Notation

A	amplitude of the sinusoidal loading history
Δu_w	excess pore water pressure build-up
$\Delta u_{w,m}$	excess pore water pressure build-up measured at the end of each load cycle
e^*_{100} , e^*_{1000}	intrinsic void ratios at 100 kPa and 1000 kPa
E_u	unloading secant Young's modulus
ε_{ax}	axial strain
$\varepsilon_{ax,l}$, $\varepsilon_{ax,g}$	local and global axial strain measurements
$\varepsilon_{ax,m}$	mean axial strain
$\dot{\varepsilon}_{ax}$	axial strain rate
$\overline{\varepsilon}_{ax,c}$	average axial strain applied in one quarter of a stress-controlled cyclic loading
$\overline{\dot{\varepsilon}}_{ax,c}$	average axial strain rate applied under stress-controlled cyclic loading
N	number of cycles
N_f	number of cycles to failure
PI	Plasticity Index
p'	effective confining pressure
p'_0	effective confining pressure at the end of the consolidation stage
q	deviatoric stress
q_0	deviatoric stress at the end of the consolidation stage
q_{max} , q_{mean} , q_{min}	maximum, mean and minimum deviatoric stress of the sinusoidal loading history
T	period of the sinusoidal loading history
σ'_v	effective vertical stress
σ'_{v0} , σ'_{h0}	vertical and horizontal in situ effective stresses
σ'_{vy}	yield stress value under oedometric conditions
w	water content
w_L , w_P	liquid and plastic limit
W_{cyc}	strain energy dissipated within one loading cycle
YSR	yield stress ratio as defined by Burland (1990)

CRediT author statement

Andrea Ciancimino: Conceptualization, Methodology, Investigation, Data Curation, Writing - Original Draft, Visualization

Renato Maria Cosentini: Methodology, Writing - Review & Editing

Sebastiano Foti: Supervision, Writing - Review & Editing, Project administration, Funding acquisition

Giorgio Volonté: Writing - Review & Editing, Project administration

Guido Musso: Conceptualization, Supervision, Methodology, Writing - Review & Editing

Declaration of competing interest

The authors declare that they have no known competing financial interests or personal relationships that could have appeared to influence the work reported in this paper.

Data availability

Data will be made available upon reasonable request.

Acknowledgments

Funding was provided by ENI SpA within the project “Hynergy”. The authors gratefully thank Eni SpA for the authorization to publish this work. The Authors would like to express their gratitude to Giampiero Bianchi for his invaluable support and assistance in running the experimental campaign.

References

Ahmadi-Naghadeh, R., Liu, T., Vinck, K., Jardine, R. J., Kontoe, S., Byrne, B. W., & McAdam, R. A. (2022). A laboratory characterisation of the response of intact chalk to cyclic loading. *Géotechnique*, 1-13.

Al-Bazali, T., Zhang, J., Chenevert, M. E., & Sharma, M. M. (2008). Experimental and numerical study on the impact of strain rate on failure characteristics of shales. *Journal of Petroleum Science and Engineering, 60*(3), 194-204. doi:https://doi.org/10.1016/j.petrol.2007.09.001

Amorosi, A., & Rampello, S. (2007). An experimental investigation into the mechanical behaviour of a structured stiff clay. *Géotechnique, 57*(2), 153-166. doi:10.1680/geot.2007.57.2.153

ASTM (2020). D4767-11 Standard Test Method for Consolidated Undrained Triaxial Compression Test for Cohesive Soils. ASTM International. West Conshohocken, PA.

Banks, D. C., Strohm Jr, W. E., De Angulo, M., & Lutton, R. J. (1975). Study of clay shale slopes along the Panama Canal - Report 3. Engineering analyses of slides and strength properties of clay shales along the Gaillard Cut (Rep S-70-9). Vicksburg, Miss.

Bardanis, M. (2024). Direct Shear Testing of Various Hard Soils and Weak Rocks from Greece. *Geotechnical and Geological Engineering*. doi:10.1007/s10706-023-02726-9

Barla, G., Barla, M., & Debernardi, D. (2010). New triaxial apparatus for rocks. *Rock Mechanics and Rock Engineering, 43*(2), 225-230. doi:10.1007/s00603-009-0076-7

Baudet, B., & Stallebrass, S. (2004). A constitutive model for structured clays. *Géotechnique, 54*(4), 269-278. doi:10.1680/geot.2004.54.4.269

Benetatos, C., Rocca, V., Verga, F., Adinolfi, L., & Marzano, F. (2023). Deformation behavior of a regional shale formation from integrated laboratory and well data analysis: insights for underground fluid storage in northern Italy. *Geoenergy Science and Engineering, 229*, 212109. doi:https://doi.org/10.1016/j.geoen.2023.212109

Bernier, F., Li, X. E., & Bastiaens, W. (2007). Twenty-five years' geotechnical observation and testing in the Tertiary Boom Clay formation. *Géotechnique, 57*(2), 229-237. doi:10.1680/geot.2007.57.2.229

Burland, J. B. (1990). On the compressibility and shear strength of natural clays. *Géotechnique, 40*(3), 329-378. doi:10.1680/geot.1990.40.3.329

Burland, J. B., Rampello, S., Georgiannou, V. N., & Calabresi, G. (1996). A laboratory study of the strength of four stiff clays. *Géotechnique, 46*(3), 491-514.

Cerfontaine, B., & Collin, F. (2018). Cyclic and Fatigue Behaviour of Rock Materials: Review, Interpretation and Research Perspectives. *Rock Mechanics and Rock Engineering, 51*(2), 391-414. doi:10.1007/s00603-017-1337-5

Chen, Z., Morgenstern, N. R., & Chan, D. H. (1992). Progressive failure of the Carsington Dam: a numerical study. *Canadian Geotechnical Journal, 29*(6), 971-988. doi:10.1139/t92-107

Ciancimino, A., Cosentini, R., Foti, S., Messori, A., Ullah, H., Volonté, G., & Musso, G. (2024). A preliminary investigation on the mechanical behaviour of a stiff Italian clay in the context of hydrogen storage. *Geomechanics for Energy and the Environment, 38*. doi:https://doi.org/10.1016/j.gete.2024.100562

Clayton, C., & Serratrice, J. (1993). The mechanical properties and behaviour of hard soils and soft rocks.

Cotecchia, F., & Chandler, R. J. (1997). The influence of structure on the pre-failure behaviour of a natural clay. *Géotechnique, 47*(3), 523-544. doi:10.1680/geot.1997.47.3.523

Cotecchia, F., & Chandler, R. J. (2000). A general framework for the mechanical behaviour of clays. *Géotechnique, 50*(4), 431-447. doi:10.1680/geot.2000.50.4.431

Fuenkajorn, K., & Phueakphum, D. (2010). Effects of cyclic loading on mechanical properties of Maha Sarakham salt. *Engineering Geology, 112*(1), 43-52. doi:https://doi.org/10.1016/j.enggeo.2010.01.002

Gasparre, A., Nishimura, S., Coop, M. R., & Jardine, R. J. (2007). The influence of structure on the behaviour of London Clay. *Géotechnique, 57*, 19-31. doi:10.1680/geot.2007.57.1.19

Gens, A. (2013). *On the hydromechanical behaviour of argillaceous hard soils-weak rocks.* Paper presented at the Proceedings of the 15th European conference on soil mechanics and geotechnical engineering.

He, M., Li, N., Zhu, C., Chen, Y., & Wu, H. (2019). Experimental investigation and damage modeling of salt rock subjected to fatigue loading. *International Journal of Rock Mechanics and Mining Sciences, 114*, 17-23. doi:10.1016/j.ijrmms.2018.12.015

Heinemann, N., Booth, M. G., Haszeldine, R. S., Wilkinson, M., Scafidi, J., & Edlmann, K. (2018). Hydrogen storage in porous geological formations - onshore play opportunities in the midland valley (Scotland, UK). *International Journal of Hydrogen Energy, 43*(45), 20861-20874. doi:10.1016/j.ijhydene.2018.09.149

Hettema, M. H. H., Schutjens, P. M. T. M., Verboom, B. J. M., & Gussinklo, H. J. (2000). Production-induced compaction of a sandstone reservoir: The strong influence of stress path. *SPE Reservoir Evaluation and Engineering, 3*(4), 342-347. doi:10.2118/65410-PA

Jeanne, P., Zhang, Y., & Rutqvist, J. (2020). Influence of hysteretic stress path behavior on seal integrity during gas storage operation in a depleted reservoir. *Journal of Rock Mechanics and Geotechnical Engineering, 12*(4), 886-899. doi:https://doi.org/10.1016/j.jrmge.2020.06.002

Ladd, C. C. (1965). *Stress-strain behaviour of anisotropically consolidated clay during undrained shear.* Paper presented at the Proc. of 6th Int. Conf. on Soil Mechanics and Foundation Engineering, Montreal.

Lavrov, A. (2016). *Dynamics of stresses and fractures in reservoir and cap rock under production and injection.* Paper presented at the Energy Procedia.

Lefebvre, G., & LeBoeuf, D. (1987). Rate effects and cyclic loading of sensitive clays. *Journal of Geotechnical Engineering, 113*(5), 476-489.

Leonards, G. A., & Altschaeffl, A. G. (1964). Compressibility of Clay. *Journal of the Soil Mechanics and Foundations Division, 90*(5), 133-155. doi:doi:10.1061/JSFEAQ.0000649

Leroueil, S., & Vaughan, P. R. (1990). The general and congruent effects of structure in natural soils and weak rocks. *Géotechnique, 40*(3), 467-488. doi:10.1680/geot.1990.40.3.467

613 Lisjak, A., Grasselli, G., & Vietor, T. (2014). Continuum-discontinuum analysis of failure mechanisms around
614 unsupported circular excavations in anisotropic clay shales. *International Journal of Rock Mechanics*
615 *and Mining Sciences, 65*, 96-115. doi:10.1016/j.ijrmms.2013.10.006

616 Mesri, G., & Shahien, M. (2003). Residual shear strength mobilized in first-time slope failures. *Journal of*
617 *Geotechnical and Geoenvironmental Engineering, 129*(1), 12-31. doi:10.1061/(ASCE)1090-
618 0241(2003)129:1(12)

619 Mohajerani, M., Delage, P., Monfared, M., Tang, A. M., Sulem, J., & Gatmiri, B. (2011). Oedometric
620 compression and swelling behaviour of the Callovo-Oxfordian argillite. *International Journal of Rock*
621 *Mechanics and Mining Sciences, 48*(4), 606-615. doi:10.1016/j.ijrmms.2011.02.016

622 Parry, R. H. G., & Nadarajah, V. (1974). Observations on Laboratory Prepared, Lightly Overconsolidated
623 Specimens of Kaolin. *Géotechnique, 24*(3), 345-357. doi:10.1680/geot.1974.24.3.345

624 Potts, D. M., Dounias, G. T., & Vaughan, P. R. (1990). Finite element analysis of progressive failure of
625 Carsington embankment. *Géotechnique, 40*(1), 79-101. doi:10.1680/geot.1990.40.1.79

626 Potts, D. M., Kovacevlc, N., & Vaughan, P. R. (1997). Delayed collapse of cut slopes in stiff clay. *Géotechnique,*
627 *47*(5), 953-982. doi:10.1680/geot.1997.47.5.953

628 Sharma, S. S., & Fahey, M. (2003a). Degradation of Stiffness of Cemented Calcareous Soil in Cyclic Triaxial
629 Tests. *Journal of Geotechnical and Geoenvironmental Engineering, 129*(7), 619-629.
630 doi:doi:10.1061/(ASCE)1090-0241(2003)129:7(619)

631 Sharma, S. S., & Fahey, M. (2003b). Evaluation of cyclic shear strength of two cemented calcareous soils.
632 *Journal of Geotechnical and Geoenvironmental Engineering, 129*(7), 608-618.

633 Skempton, A. (1954). The pore-pressure coefficients A and B. *Géotechnique, 4*(4), 143-147.

634 Skempton, A. W. (1969). The consolidation of clays by gravitational compaction. *Quarterly Journal of the*
635 *Geological Society of London, 125*(1-4), 373-408. doi:10.1144/gsjgs.125.1.0373

636 Smith, P. R., Jardine, R. J., & Hight, D. W. (1992). The yielding of Bothkennar clay. *Géotechnique, 42*(2), 257-
637 274. doi:10.1680/geot.1992.42.2.257

638 Sone, H., & Zoback, M. D. (2014). Time-dependent deformation of shale gas reservoir rocks and its long-term
639 effect on the in situ state of stress. *International Journal of Rock Mechanics and Mining Sciences, 69*,
640 120-132. doi:https://doi.org/10.1016/j.ijrmms.2014.04.002

641 Tavenas, F., Leroueil, S., Rochelle, P. L., & Roy, M. (1978). Creep behaviour of an undisturbed lightly
642 overconsolidated clay. *Canadian Geotechnical Journal, 15*(3), 402-423. doi:10.1139/t78-037

643 Teatini, P., Castelletto, N., Ferronato, M., Gambolati, G., Janna, C., Cairo, E., . . . Bottazzi, F. (2011).
644 Geomechanical response to seasonal gas storage in depleted reservoirs: A case study in the Po River
645 basin, Italy. *Journal of Geophysical Research: Earth Surface, 116*(2). doi:10.1029/2010JF001793

646 Terzaghi, K. (1941). Undisturbed clay samples and undisturbed clays. *J. Boston Soc. Civ. Eng., 28*, 211-231.

647 Ushev, E., & Jardine, R. (2022). The behaviour of Bolders Bank glacial till under undrained cyclic loading.
648 *Géotechnique, 72*(1), 1-19. doi:10.1680/jgeot.18.P.236

649 Vaid, Y. P., & Campanella, R. G. (1977). Time-dependent behavior of undisturbed clay. *Journal of the*
650 *Geotechnical Engineering Division, 103*(7), 693-709.

651